Aalborg Universitet

Robust High-Rate Secondary Control of Microgrids with Mitigation of Communication Impairments

Heydari, Rasool; Khayat, Yousef; Amiri, Abolfazl; Dragicevic, Tomislav; Shafiee, Qobad; Popovski, Petar; Blaabjerg, Frede

Robust High-Rate Secondary Control of Microgrids with Mitigation of Communication Impairments

Rasool Heydari, *Member, IEEE,* Yousef Khayat, *Student Member, IEEE* Abolfazl Amiri,
Tomislav Dragicevic, *Senior Member, IEEE,* Qobad Shafiee, *Senior Member, IEEE,* Petar Popovski, *Fellow, IEEE,*
and Frede Blaabjerg, *Fellow, IEEE*

Abstract—The dynamic response speed of the secondary control (SC) in microgrids (MGs) is limited both by the communication network time delays and the bandwidth (BW) of the primary control (PC). By increasing the PC BW, which depends on how to design and tune the PC, the time delay issues will be multiplied due to the speed range of the communication modules and technologies. This paper proposes a communication compensation block (CCB) to enhance the robustness of distributed SC against communication impairments in the MGs operated at the higher BW. The proposed method mitigate malicious time delays and communication non-ideality in distributed networked controls employed in the secondary layer of the MG by prediction, estimation and finally decision on transmitted data. A comprehensive mathematical model of the employed communication network is presented in details. Then, a robust data prediction algorithm based on the temporal and spatial correlation is applied into the SC to compensate for time delays and data packet loss. Furthermore, the effect of the number of stored packets and burst packet loss on the average success rate of the communication block, and the small signal stability analysis of the system in the presence of the CCB are investigated. Power hardware-in-the-loop (PHiL) experimental tests show the merits and applicability of the proposed method.

Index Terms—Communication compensation, data packet loss, distributed control, model predictive control, secondary control.

I. INTRODUCTION

THE microgrids (MGs) have been introduced as a promising, effective, and efficient way to utilize distributed generation of renewable resources either in remote areas where the physical interconnection with the main utility is not conceivable, or in the new distributed power systems. Though the MGs can be employed in grid connected mode, islanded operation of them is an inevitable operation situation due to intentional or unintentional conditions. To ensure the control of MG dynamics, a hierarchical control structure including primary control (PC), secondary control (SC), MG emergency/central control (MGCC), and global control have been proposed [1].

PC level deals with stabilizing the voltage and frequency values adjusted by droop mechanism. The frequency and

R. Heydari is with Electrical Engineering, Mads Clausen Institute, University of Southern Denmark, Odense, DK, 5230, Denmark, e-mail: (rah@mci.sdu.dk).

Y. Khayat, T. Dragicevic and F. Blaabjerg are with the Department of Energy Technology, Aalborg University, Aalborg, DK, 9220, Denmark (e-mail: tdr@et.aau.dk, fbl@et.aau.dk).

A. Amiri and P. Popovski are with the Department of Electronic Systems, Aalborg University, Aalborg, DK, 9220, Denmark (e-mail: aba@es.aau.dk, petarp@es.aau.dk).

Q. Shafiee is with the Department of Electrical Engineering, University of Kurdistan, Sanandaj, Iran (e-mail: q.shafiee@uok.ac.ir)

voltage amplitude are stabilized through inner control loops following by the frequency and voltage set points adjusted by droop mechanism. Droop control is a communication-free power sharing mechanism inspired by the synchronous generators in the conventional power systems [2], [3]. Steady state deviations in the frequency and voltage set-point is the main drawback of this mechanism, hence, at the upper level, SC is implemented to compensate for the steady state errors caused by the droop [3]–[7].

The SC can be implemented in a centralized [8], distributed [9], or decentralized structure [10]. Due to the single point of failure of the centralized SC, which leads to a collapse in the SC level, this structure is not a proper choice for reliable operation of the MG. Thus, as an alternative, the distributed SC structure has been presented [4], [11]. Averaging [12]–[15] and consensus [11], [16]–[22] are two other architectures to realize the distributed SC.

Most of the reviewed distributed structures rely on the linearized cascaded control loops, which suffer from several inherent limitations. In such structures, every outer loop is designed to have an order of magnitude slower response and smaller BW compared to the inner control loops. It leads to the overall slow dynamic performance and severe voltage and frequency deviations. Furthermore, accurate transient power sharing is not satisfied in the conventional approach. Therefore, a new approach based on the model predictive control (MPC) of power converters is presented in [23], in which rapid transient response and robust control technique is demonstrated. In [24], [25] a high BW SC applying finite control set MPC is presented. However, it relies critically on the assumption of ideal communication links. It is therefore of interest to investigate the impact of data packet losses and time delays on the accuracy of the high BW control structure.

Any wireless communication technology employed in distributed control of MGs to exchange information among DGUs, such as Wi-Fi or LTE/4G, inevitably introduces delays and packet losses [8], [26], [34], [35]. Besides the delay, the MG control performance can also be affected by the sampling rates of communication modules. However, sampling rates of communication modules and technologies are very fast, for instance Wired Ethernet networked systems have Megabits data rates, Wireless Ethernet systems have Gigabit data rates, and Power Line Communication technology utilizes 9600 to 19200 bit/s overall sampling rate. In contrast, the data volume of the SC signals in a fast frequency and voltage restoration might challenge the system with time delays [36]. Thus, the main focus of this paper is the impact of the communication impairments on the fast SC implementation. In fact, most

TABLE I. MG Communication Uncertainties and Time Delays Literature.

Ref.	Main Contribution	Complexity	Physical Insight	Necessity of Assumption	Controller type	Restoration time
[8]	Calculate delay margins	Low	Medium	High	Gain-scheduling	$\approx$ 2 Seconds
[21]	Estimates MG states	High	High	Low	Nonlinear	$\approx$ 50 Seconds
[26]	Stability analysis	Low	High	Low	PI	$\approx$ 2 Seconds
[27]	Stability enhancement	High	Medium	Low	PI	–
[28]	Optimization-based information sharing	High	Medium	High	Adaptive	$\approx$ 4 Seconds
[29]	Considers model of time delays	Low	Medium	low	MPC	$\approx$ 5 Seconds
[30]–[33]	Design issues of network architecture	Medium	High	Low	PI - PID	

of the reported literature [9] have only addressed the slow SC for a MG with conventional PC including voltage and current loops. Table I. shows a comprehensive overview of communication non-idealities compensation presented in the literature.

According to the studies in [37], [38] and experimentally evaluated in [14], based on IEEE 802.11 (Wi-Fi), the minimum time interval for information update is 10 ms. Hence, to enhance the dynamic performance of the MG, not only PC and SC should be designed with higher BW, but communication delay and packet loss, which degrade the system performance much drastically in higher rate operation, should also be considered. Existing reports and literature have overlooked the communication delays, while, a systematic time-delay study, which proposes a solution for communication impairments, is still missing.

Recently, a comprehensive overview on the SC architectures has been presented in [39], where, in a general classification, centralized, distributed, and decentralized approaches have been introduced as three main SC architectures. In distributed SCs, which are focused in this paper, how to address a controller such that provides a robust performance against time-delays is introduced as a key challenge in [39]. In addition, the importance of communication infrastructure in different perspectives for cyber-physical power-electronic base generation systems like ac and dc MGs, has been shown in [40]–[42]. In cyber-physical systems, designing appropriate approaches to cope with the cyber-attack for a resilience cyber-operation has also been becoming popular, as presented in the recent researches such as [43]–[45]. To address this, a cyber-physical design is recommended for the cyber-physical MG systems. Most of the recommended designs are based on this fact on how we can incorporate the cyber disturbances in the SC, however, a promising solution to fill this gap can be addressed by a communication compensation block (CCB), as we have focused on it, in this paper.

In this paper, a CBB is proposed to be implemented into the distributed SC to compensate for communication delay and packet loss. The major contributions of this approach are:

1) A systematic procedure to design a CCB for communication impairments in distributed cooperative SC applied to an islanded MG is proposed.

2) By employing the proposed CCB, the SC properly regulates the voltage and frequency at the higher BW and order of magnitudes faster than the state of the art, even in the presence of communication impairments. Furthermore, the

proposed CCB protocol meets the power sharing accuracy in the presence of communication uncertainties.

3) The proposed CCB utilizes a data prediction unit, which makes the SC exceptionally robust to data packet loss and communication impairments.

4) From the practical perspective, communication impairments and the MG parameters, such as line impedance, loads, and the MG configuration are unknown. Unlike existing distributed methods that require a detailed model of the MG, the proposed protocols are designed by considering unmodeled communication dynamics, unknown delays, packet loss and impairments. Therefore, the controllers can be designed independent of the DG parameters and communication uncertainties.

The rest of this paper is organized as follows. Section II presents a brief introduction to conventional low BW primary control, high BW finite control set MPC (FCS-MPC), their time-scales, and SC function. Details of the proposed data prediction and communication compensation algorithm are given in Section III. In Section IV, small signal analysis and stability of the proposed high BW control scheme is presented. Simulation and experimental results of the proposed approach are demonstrated in Section V. Finally, Section VI concludes the paper.

II. DISTRIBUTED HIERARCHICAL CONTROL STRUCTURE

The dynamic response speed of the SC can be enhanced by appropriate tuning of the controller parameters. However, it is limited both by the communication network time delays and the BW of the PC. In the conventional PC, multi-linearized cascaded control loops ensure the voltage and frequency stability. It comprises inner voltage and current control loops, as well as droop controller. This cascaded control structure suffers from the inherent slow dynamic response since the outer loops should be designed with approximately an order of magnitude lower BW compared to the inner one [25]. Therefore, the BW of the PC level limits the SC BW.

A. Primary Control (PC)

Fig. 1(a) shows the approximate BW of each control loop in a cascaded multi-loop control structure. In order to address the slow dynamic response problem, inner voltage and current controllers are replaced with a single FCS-MPC [23], [25]. It increases the system frequency BW and fast control response. Fig. 1(b) shows the BW improvement of FCS-MPC structure. Therefore, the SC can be design with higher BW. In this
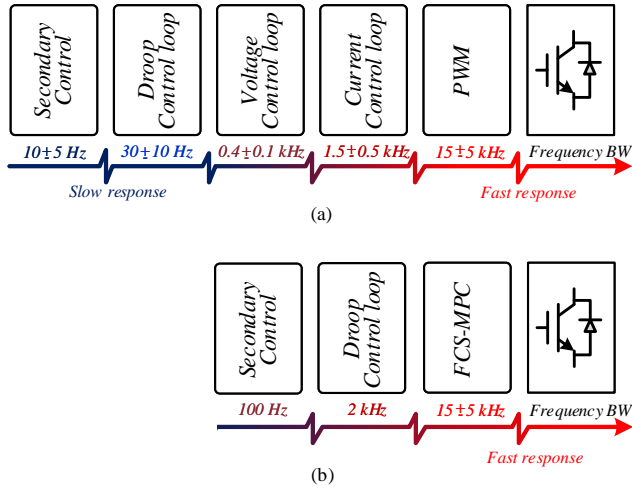
Fig. 1. A frequency bandwidth (BW) comparison between (a) conventional cascaded control structure and (b) FCS-MPC based control approach.

approach, the future state of the variables is obtained by exploiting the system model and minimizing a predefined cost function.

Considering a three phase VSC connected to the AC bus through an LC filter. The switching network (6 switches) can be obtained by three main gating signals i.e. S_a, S_b, and S_c. The objective of FCS-MPC is to calculate the cost function for all possible switching states, then, apply the switching configuration corresponding the voltage vector V_i, which minimize the cost function. The cost function (CF) is expressed as follows [23], [25]:

$$CF : \|\overline{v}_e(i)\|^2 + \lambda_{der} g_{der}(i) + h_{lim}(i) + \lambda_s sw^2(i), \quad (1)$$

$$\overline{v}_e(i) = (v^*_{f\alpha} - v_{f\alpha})^2 - (v^*_{f\beta} - v_{f\beta})^2, \quad (2)$$

$$g_{der}(i) = \left(\frac{d\overline{v}^*_f(t)}{dt} - \frac{d\overline{v}_f(t)}{dt} \right) = (C_f \omega_{ref} v^*_{f\beta} - i_{f\alpha} + i_{o\alpha})^2 + (C_f \omega_{ref} v^*_{f\alpha} + i_{f\beta} - i_{o\beta})^2, \quad (3)$$

$$h_{lim}(i) = \begin{cases} 0, & \text{if } |i_f(i)| \le i_{max} \\ \infty, & \text{if } |i_f(i)| > i_{max} \end{cases}, \quad (4)$$

$$sw(i) = \sum |u(i) - u(i-1)|. \quad (5)$$

where $\overline{v}_e(i)$ stand for the Euclidean distance between reference voltage (v^*_f) and the predicted value (v_f) in the $\alpha - \beta$ frame, formulated in (2). To decrease the total harmonic distortion (THD), another term (g_{der}) with a weighting factor (λ_{der}) is added to the cost function, hence, the output voltage follows the voltage reference trajectory and its derivative simultaneously [23], [24]. $h_{lim}(i)$ and sw express the current constraint, and the switching effort with a weighting factor (λ_s), respectively. Compared to the conventional multi-loop cascaded control, the mentioned FCS-MPC based structure has much faster dynamic performance.

B. Secondary Control

Typically, conventional SC parameters are selected to result in lower BW in order not to have any interaction with PC loops, hence, slow dynamic response in primary loops leads to a sluggish response of overall system. By implementing the FCS-MPC, there is no filtering necessary in the primary loops, nor there exists low pass filtering behaviour of conventional cascaded linear loops, thus, the SC can be operated with higher BW (see Fig. 1).

Based on the graph theory and cooperative team objectives in consensus protocol [46], the following distributed SC correction terms are provided for frequency and voltage control.

In order to compensate for frequency and voltage deviations, a complementary signal is deployed to the droop to adjust the reference value. The compensating signal can be achieved as follows:

$$\begin{cases} \omega_{ref} = \omega_{nom} + m_q Q + \delta^\omega_{DG_i} \\ V_{ref} = V_{nom} - m_p P + \delta^v_{DG_i} \end{cases}, \quad (6)$$

while (6) is the $\omega - Q$ and $v - P$ droop characteristic, δ_{DG_i} represents compensating signal sent to the primary control to adjust the frequency and the voltage amplitude reference. It is worth to note that a virtual resistive impedance is employed to enforce the output impedance, seen by VSC, to be purely resistive, hence, the line impedance (resistive or inductive) cannot affect the accuracy of the control strategy [47]. The SC compensating signal is as follows:

$$\delta_{DG_i} = K_i(s) \sum_{j \in \mathcal{N}, j \neq i} \alpha_{ij}(x_j(t) - x_i(t)), \quad (7)$$

where, $K_i(s)$ is the controller, and α_{ij} is the communication graph adjacency matrix arrays, i.e., α_{ij} indicates whether the DG_i and DG_j are adjacent or not.

It is worth to note that a high rate communication network is required to share data (voltage and frequency) at the upper level.

III. PROPOSED COMMUNICATION COMPENSATION ALGORITHM

Regarding the communication link between secondary controller and using wireless communications to access this medium, it is convenient to use well-known protocols. Here, the IEEE 802.11 (WiFi) standard is selected for the communication infrastructure in regards to the delay and reliability constraints in the system model. Since the main objective of this paper focuses on fast response to load changes within the network, a user datagram protocol (UDP) is incorporated into the transmission layer [48]. The UDP cannot enter into a heavily delayed state due to multiple queued transmissions.

Practical properties of the WiFi described in [49] can fulfil the requirements demanded by our system model. Latency and reliability measurements show that this technology provides relatively high reliability (around 95%) within a very short delay (less than 1 ms) for a packet size of 1500 bytes. On the other hand, while the packet size is smaller in our model (512 bytes), then the results are certainly valid for 512 bytes (one can simply pad the 512 bytes with zeros and get packets
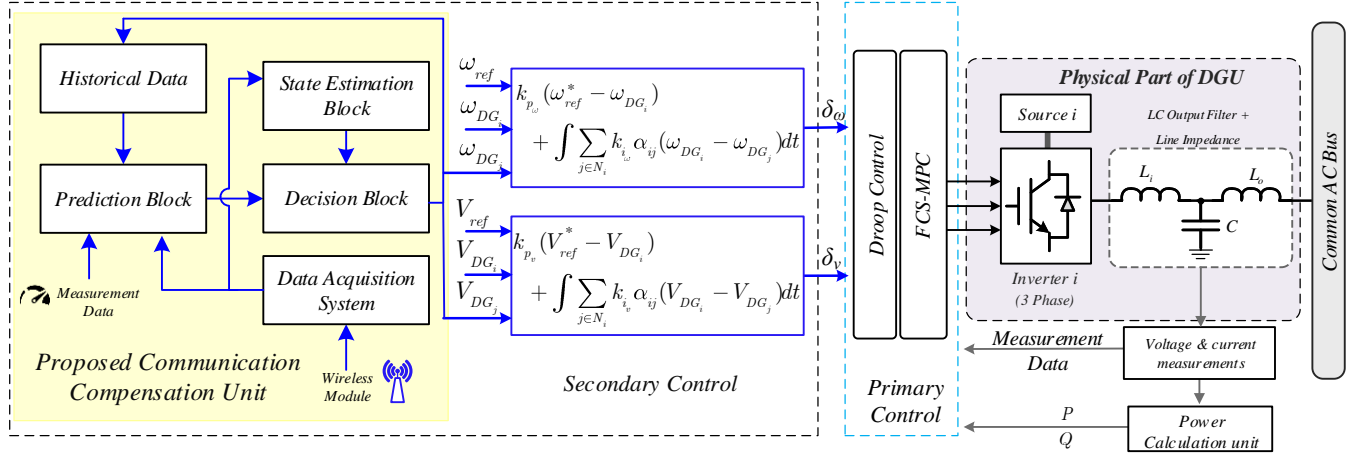
Fig. 2. Detailed schematic of proposed control structure with communication compensation.

of 1500 bytes). However, the scenario in this system is not ultra-reliable and low-latency communication (URLLC) [50] since it can enjoy more relaxed latency constrains and lower error-rates (or reliability). This indeed gives more degrees of freedom for the communication link design. Here we want to use off-the-shelf components, while URLLC from 5G is still in development.

A. Prediction Block

In this section, mathematical model of communication block, shown in Fig. 2, is described in details.

Consider the transmitting data from ith unit in the kth time slot to be $x_i^j(k)$, where $j \in \{v, f\}$ denotes the voltage and frequency data respectively.

Assuming that the system loses data packet $x_i^j(k)$ during the transmission and the objective is to recover this loss within the system. Recovery processes are done due to temporal and spatial correlation properties of the data packets. Thus, the lost packets are reconstructed based on the stored information which can be formulated as:

$$
\begin{aligned}
x_i^j(k) =& \alpha \mathcal{F}(x_i^j(k-n)|n \in \{1,\dots,N\}) \\
& + (1-\alpha)\mathcal{G}(x_m^j(k)|m \in \{1,\dots,M\}, m \neq i),
\end{aligned} \quad (8)
$$

where, $\mathcal{F}(.)$ determines the temporal dependency of $x_i^j(k)$ with previous data of DG$_i$. $\mathcal{G}(.)$ shows the spatial reliance of $x_i^j(k)$ in all the data from other neighbour DGs in the power system network. Also, N and M are memory stack size and number of all neighbour DGs with DG$_i$. The size of historical data memory size is a parameter depending on the quality of the wireless channel. Finally, a weighting factor α is used to balance the data fusion between the mentioned functions.

Concerning the storage and recalling of the data for the prediction analysis, two blocks are used. The first one, *Historical Data*, is in charge of storing measurement data of each DGs own data. In other words, it is a data memory of size N and keeps the last N output of the communication block. Next is *Data Acquisition System* that extracts data from other neighbour DGs and sends it to the prediction block for further computations.

In general, $\mathcal{F}$ and $\mathcal{G}$ can have any sort of complex formulation, but in order to reduce the complexity of the practical

structure, linear models are utilized to characterize them. Hence,

$$
x_i^j(k) = \alpha \frac{1}{N} \sum_{n=1}^{N} \omega_n^j x_i^j(k-n) + (1-\alpha) \sum_{l=1, l \neq i}^{M} \psi_l^j x_l^j(k). \quad (9)
$$

Here, the ultimate goal is to find values of ω_n^j, ψ_l^j and α to minimize the prediction error. The concept of correlation in the data sources is used to derive a linear relation for the aforementioned functions. Next, a non-linear Mean Square (MS) method for a regression model over each correlation function is employed. Then, the lost data are reconstructed and recovered according to the data set from the DG$_i$ itself and its neighbour DGs in the network.

Starting with $\mathcal{F}$ and Auto-Correlation Function (ACF) of x_i^js which is,

$$
ACF(x_i^j, n) = \sum_{k=-\infty}^{\infty} x_i^j(k) x_i^j(k-n), \quad (10)
$$

where it is assumed that the measured data are non-complex. Furthermore, applying a non-linear MS regression method ACF can be modelled as an exponential model as the following,

$$
ACF(x_i^j, n) = a \exp(-\frac{x_i^j - b}{c}), \quad (11)
$$

where, values of a, b and c are derived to minimize the MS error. In order to find ω_n^j, ACF should be related with previous data of the DG. Therefore, with a least square linear prediction approach, this relation is as the following,

$$
x_i^j(k) = \mu(1 - ACF(x_i^j, n)) + ACF(x_i^j, n) x_i^j(k-n), \quad (12)
$$

in which, μ is stationary average of x_i^js. Putting together (11) and (12) results in

$$
\omega_n^j = \frac{x_i^j(k)}{x_i^j(k-n)} = ACF(x_i^j, n) + \frac{\mu(1 - ACF(x_i^j, n))}{x_i^j(k-n)} \quad (13)
$$

$$
= a \exp(-\frac{n-b}{c}) + \frac{\mu(1 - a \exp(-\frac{n-b}{c}))}{x_i^j(k-n)}. \quad (14)
$$

The same procedure can be executed for the $\mathcal{G}$ function as well. Thus, ψ_l^js can be written as:

$$\psi_l^j = \frac{x_l^j(k)}{x_i^j(k)} = a' \exp\left(\frac{-x_l^j(k) + b'}{c'}\right)$$

$$+ \frac{\mu'(1 - a' \exp(\frac{-x_i^l(k)+b'}{c'}))}{x_l^j(k)} \quad (15)$$

where, a', b' and c' are coefficients of the regression function over cross-correlation between $x_i^j(k)$ and $x_l^j(k)$. Moreover, μ' is the average value of $x_l^j(k)$s. In order to have a simpler model, it is assumed that the ψ_l^j only depends inversely on the distance between DG_i and DG_l, which are obtained from GIS data. Regarding the value of α, since the reliance between the data within a DG is larger than its value among other DGs, it is straightforward that $\alpha > 0.5$. Finally, by substituting all the parameters in (9) and using (14) and (15), a complete predictive model is attained for the system.

B. State Estimation Block

This block is in charge of estimating the system state information, which employed a two dimensional Markov chain following a Gilbert-Elliot structure. Generally, prediction model deals with four types of states which are depicted in Fig. 3. These states depend on two variables that control the outcome of the communication block. The first variable is the condition with the power system implying whether it is operating in a (i) *normal state* or (ii) *transient state*. The first one is the expected operational state of the power system while the later one occurs when a disturbance, i.e. load change, happens within the system. The second variable indicates quality of the communication link between the units showing if it is in a (i) *normal link state* or (ii) *failed link state*. It is assumed that the packet loses happen while the system is in the failed link state. Also, since these two groups of states are independent, 4 states can describe all the variables within the system.

Fig. 3 illustrates the Markov chain governing the states of the system. For instance, a disturbance in the power system or a packet loss in the data transmission lead to state transition within the chain. It is worth mentioning that it is assumed that the probability of occurrence of both of these failures is very small and neglected. This removes the state transitions between totally normal state to the transient-link failed state. However, considering this transition probability will not change the way we solve the problem. Moreover, distribution of these transition probabilities depend on many parameters such as implementation facts of the power systems, load change models, radio environment factors and etc. A detailed analysis of this model is left for the future work.

C. Decision Block

The final impact of the communication block on the overall system is determined by this block. It chooses between the two transmission modes and also decides what to send in each of the modes. For instance, in normal transmission mode, it sends packets with $B = 512$ bits including predicted data from (9) and also regression coefficients of (14) and (15).
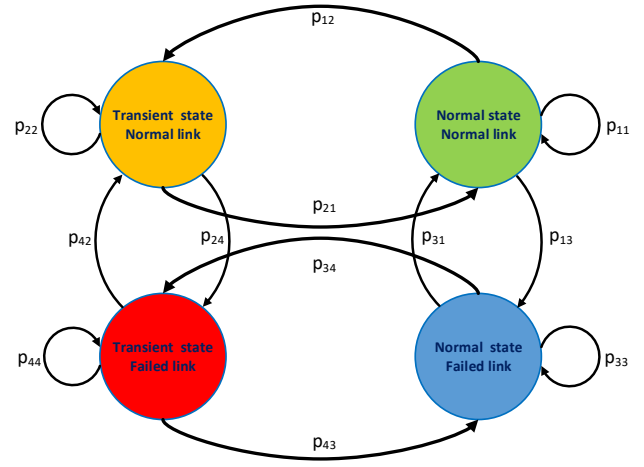

Fig. 3. Two dimensional Markov chain for the different states within the system.

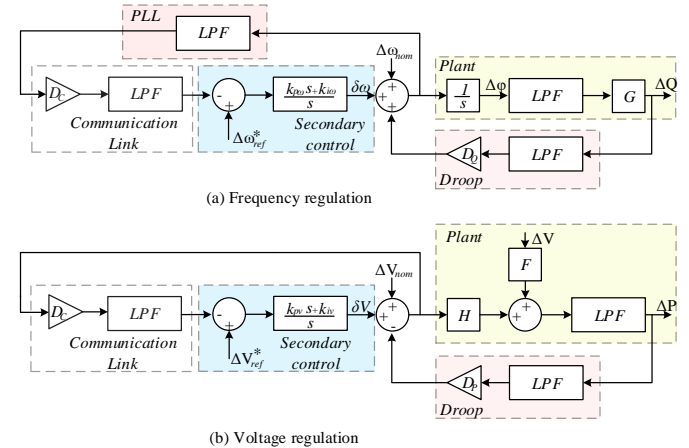(a) Frequency regulation

(b) Voltage regulation

Fig. 4. Small signal block diagram: (a) frequency regulation, and (b) voltage regulation.

IV. FREQUENCY ANALYSIS AND SMALL-SIGNAL STABILITY

In order to tune the high BW SC parameters, and perform the overall system stability analysis, a dynamic model of MG has been performed. The s-domain block diagram of MG consists of inner plant control, droop control, SC and communication link which are presented in Fig. 4. Also, a phase locked loop (PLL) is implemented in the frequency control model in order to extract the system frequency. Furthermore, a low pass filter (LPF) representing the dynamic model of control structure is employed in the plant model and also an LPF representing the dynamic model of the communication algorithm is applied in the communication block. It is worth noting that the BW of LPF should be smaller than interior loops. In order to achieve the dynamic behaviour of the LPF in the communication link a frequency analysis based on the Fourier transform is carried out.

A. Communication Link Dynamic Performance

In this part, a frequency domain analysis for the proposed prediction block is presented, to be used for stability analyses of the overall system. Considering (9), where the complete

relation of the signal to different sources is mentioned, a discrete Fourier transform is defined as,

$$X(\iota\Omega) = \sum_{k=-\infty}^{\infty} x(k) \exp^{-\iota\Omega k} \qquad (16)$$

where, k is a time variable, ι is imaginary unit and Ω is in the frequency domain. Thus, applying this transformation to (9) results in,

$$X(\iota\Omega) = \sum_{k=-\infty}^{\infty} [\alpha \frac{1}{N} \sum_{n=1}^{N} \omega_n^j x_i^j(k-n) +$$

$$(1-\alpha) \sum_{l=1, l\neq i}^{M} \psi_l^j x_l^j(k)] \exp^{-\iota\Omega k} \qquad (17)$$

Since the second term in (17) is independent of current DG's time domain, it is considered as a constant term and therefore,

$$X(\iota\Omega) = \alpha \frac{1}{N} \sum_{k=-\infty}^{\infty} \sum_{n=1}^{N} [\sum \omega_n^j x_i^j(k-n) + \Lambda] \exp^{-\iota\Omega k}$$

$$= \alpha \frac{1}{N} \sum_{k=-\infty}^{\infty} \sum_{n=1}^{N} [\sum ACF(x_i^j, n) x_i^j(k-n)$$

$$+ \mu(1 - ACF(x_i^j, n)) + \Lambda] \exp^{-\iota\Omega k} \qquad (18)$$

Here, $ACF(.)$ is time independent and therefore the second term is also constant. Then,

$$X(\iota\Omega) = \frac{\alpha}{N} \sum_{n=1}^{N} [ACF(x_i^j, n) \sum_{k=-\infty}^{\infty} (x_i^j(k-n) + \Lambda') \exp^{-\iota\Omega k}]$$

$$= \frac{\alpha}{N} \sum_{n=1}^{N} [ACF(x_i^j, n)(X(\iota\Omega) \exp^{-\iota\Omega n} + \Lambda' \delta(\iota\Omega))] \qquad (19)$$

where, Λ' is new accumulated constant and $\delta(.)$ is Dirac delta function. Finally, with a bit reordering, in can be written:

$$X(\iota\Omega) = \frac{\frac{\alpha}{N} \sum_{n=1}^{N} ACF(x_i^j, n) \Lambda' \delta(\iota\Omega)}{1 - \frac{\alpha}{N} \sum_{n=1}^{N} ACF(x_i^j, n) \exp^{-\iota\Omega n}} \qquad (20)$$

Therefore, according to delta function's features, the final form of the frequency response of the prediction block is

$$X(\iota\Omega) = \begin{cases} \frac{\frac{\alpha}{N} \sum_{n=1}^{N} ACF(x_i^j, n) \Lambda'}{1 - \frac{\alpha}{N} \sum_{n=1}^{N} ACF(x_i^j, n)} & \text{for } \Omega = 0 \\ 0 & \text{other wise} \end{cases} \qquad (21)$$

This equation concludes that the prediction block only has DC components.

B. System Delay Characteristics

One of the important design parameters in this system is the number of stored historical data N of each DG unit. This introduces additional processing delay in the whole system model. However, increasing N results in more accurate prediction model allowing better performance of the communication block's output. Therefore, this trade-off should be investigated in order to give insights over the design part of the blocks. The effect of the number of stored sampled data is well studied in (9). Here, a delay model is proposed to model lags introduced
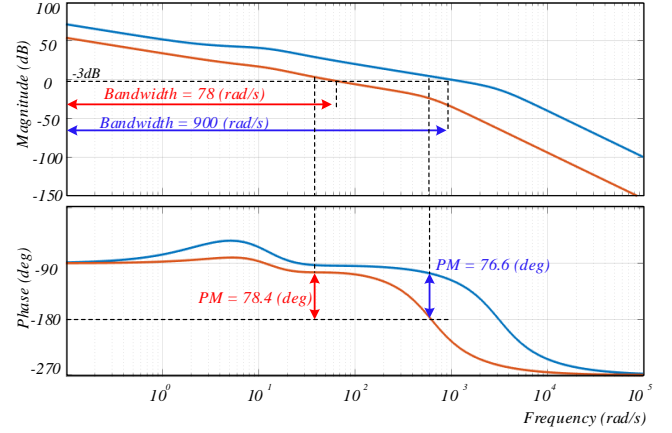

Fig. 5. Bode diagram for the conventional linear control structure (red line) and the proposed FCS-MPC based control approach (blue line).

by communication block. A general communication delay is as the following:

$$\tau_{communication} = \tau_{propagation} + \tau_{processing} + N\tau_{computation} \qquad (22)$$

where, subscripts show the reason of introduced delays. Propagation delay is the average time for transmitting wireless signal through the wireless media. Then, there is a processing delay regarding the state estimation and decision processes within the communication block. Finally, the last term in (22) shows the delay according to the prediction model and the data storage, which scales with the stack size N.

C. Stability Analysis

In order to tune the SC parameters (k_i and k_p), the system phase margin and gain margin should be in an acceptable range and the overall system should be maintained stable with fast response time. Hence, fast and accurate dynamic performance are achieved. Based on Fig. 4, and Mason's theorem, the open loop path transfer function can be derived as follows:

$$\frac{\Delta Q(s)}{\Delta \omega(s)} = \frac{\frac{Dc}{\tau_c s+1} \times \frac{k_{p\omega}s+k_{i\omega}}{s} \times \frac{1}{s} \times \frac{1}{\tau_p s+1} \times M}{1 + \frac{1}{s} \times \frac{1}{\tau_p s+1} \times M \times \frac{D_Q}{\tau_d s+1}}, \qquad (23)$$

$$\frac{\Delta P(s)}{\Delta V(s)} = \frac{\frac{Dc}{\tau_c s+1} \times \frac{k_{pv}s+k_{iv}}{s} \times N \times \frac{1}{\tau_p s+1}}{1 - \frac{1}{\tau_p s+1} \times \frac{D_p}{\tau_d s+1}}, \qquad (24)$$

where, blocks of M and N in the dynamic model block can be achieved as follows:

$$M = -\frac{V_{MG} V_i \cos \phi_i}{R_i}, \qquad (25)$$

$$N = \frac{2V_{MG} - V_i \cos \phi_i}{R_i}. \qquad (26)$$

Bode diagram for the proposed FCS-MPC approach and the conventional cascaded control structure are demonstrated

TABLE II. PARAMETERS OF THE TEST SYSTEM

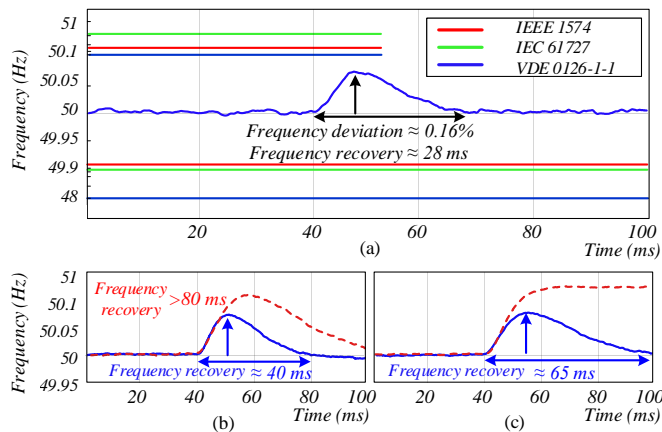| Electrical Parameters		
Parameters	Symbol	Value
Output voltage of rectifier	V_{DC}	650 V
Nominal voltage magnitude	V_i	200 V
Nominal frequency	f	50 Hz
Sampling time	T_s	25 μs
Capacitance of LC filter	C_f	25 μ F
Inductance of LC filter	L_f	2.4 mH
Virtual resistance	R_v	2 Ω
Control Parameters		
Control Parameters	DGU: 2 and 4	DGU: 1 and 3
$P - v$ droop coefficient	0.001 V/W	0.002 V/W
$Q - \omega$ droop coefficient	0.005 rad/VAr.s	0.01 rad/VAr.s

Fig. 6. Validation of the proposed networked control with (blue) and without (red) prediction block: (a) MG frequency restoration with ideal communication link, (b) frequency restoration with 20% packet loss probability, (c) frequency restoration with 60% packet loss probability.
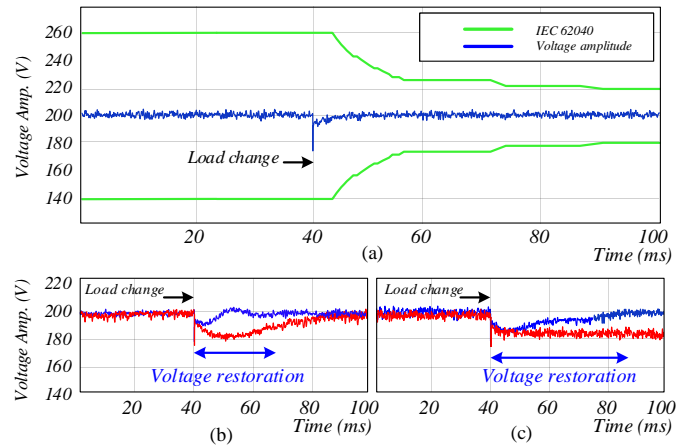

Fig. 7. Validation of the proposed networked control with (blue) and without (red) prediction block: (a) voltage regulation with ideal communication link, (b) voltage regulation with 20% packet loss probability, (c) voltage regulation with 60% packet loss probability.

ideal transmission link, the frequency is restored very fast with respect to the standards by a vast margin. Based on the IEEE 1574 standard acceptable restoration time is 160 ms and allowable deviations is 0.8% for over frequency and 1% for under frequency in the MGs [24]. Fig. 6(b), and (c) show the effect of communication impairments on control structure. Although the proposed FCS-MPC structure is robust to parameter changes [24], [51], unreliable transmission degrades the performance of the control structure. Therefore, in Fig. 6(c) with 60% packet loss, each packet can be lost independently with probability of 60%, hence, by applying a load change the SC cannot recover the MG frequency. However, by employing the proposed data prediction block in communication link the control structure compensates for packet loss and transmission deficiencies. Therefore, even with 60% non-ideal communication link, frequency deviations are compensated accurately. Fig. 7 shows the voltage amplitude control performance. As it can be seen in Fig. 7(a), the voltage is maintained stable during a load change with a vast margin of the IEC standard. However, the communication deficiencies degrade the secondary voltage control performance. Fig. 7(b) and (c) shows the secondary voltage control performance with a probability of 20% and 60% packet lost in communication link, respectively. As it can be seen, the SC cannot compensate for voltage amplitude deviations with 60% packet lost. On the other hand, by implementing the prediction block in SC, the voltage is restored even with 60% communication link non-ideality.

B. Effect of Historical Data Storage Size on the System Performance

One key factor in the design process of the communication block is to determine N which is the historical data storage size. As discussed in the previous sections, there is a trade-off point for selecting N since it both controls the system accuracy and delay. In Fig. 8, the effect of the number of stored historical packets N and burst packet lost on the average success rate of the communication block is illustrated. As it

in Fig. 5. The SC parameters are selected so that the MG stability is achieved and also the SC compensate for voltage and frequency deviations immediately.

As it can be seen, by implementing the proposed control strategy, MG can be operated in higher BW compared to the conventional linearized cascaded methods.

V. SIMULATION AND EXPERIMENTAL RESULTS

In order to verify the proposed distributed networked control structure, an islanded ac MG consists of four VSCs is implemented in MATLAB SimPower system. The reference voltage and frequency are 200 V and 50 Hz respectively. The simulated parameters can be obtained from Table II.

A. Effect of Data Packet Loss on the Control Performance

Conventionally, the control structures rely on the information exchanged. However, communication links are not ideal and degrade the performance of the control system. Some data packets suffer from communication delay and can also be dropped out during transmission. In this section, the effect of data packet losses on the proposed networked control is scrutinized. Fig. 6 demonstrates the efficiency of the proposed algorithm in the presence of communication network non-idealities. As it can be seen from Fig. 6(a), with
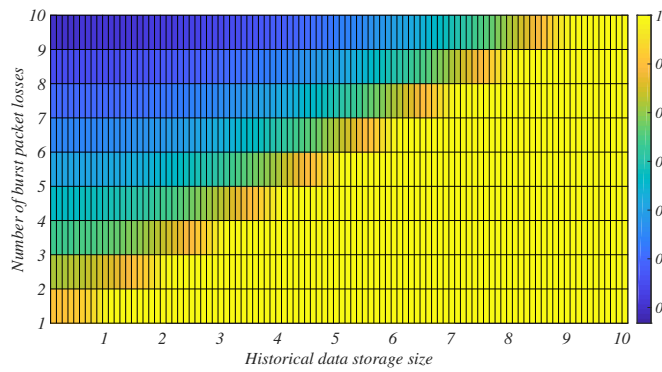
Fig. 8. The effect of the number of stored packets N and burst packet lost on the average success rate of the communication block.

Fig. 10. Active power sharing among the DGUs in the presence of the proposed secondary control.
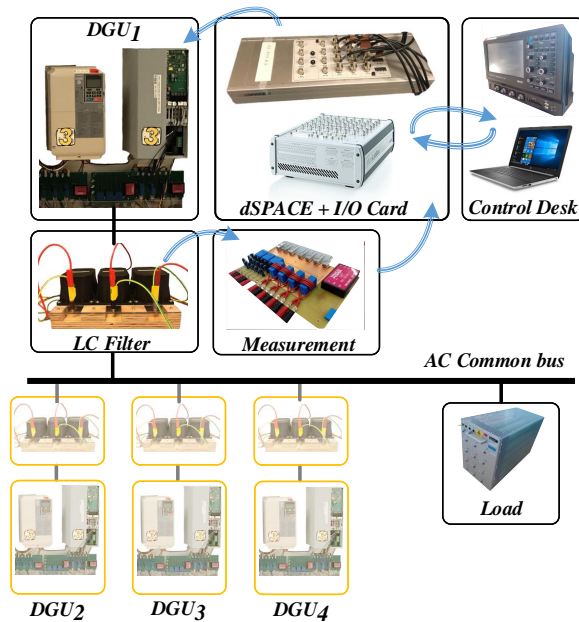

Fig. 9. Experimental setup consists of a dSPACE controller, four VSCs and filters, measurements, loads and scope.

can be seen, with a larger N system performs better in terms of packet recovery rate. However, there is a saturation point which lays on $x = y$ line meaning that storing more packets than the burst packet loss size does not improve the system performance. Therefore, it is convenient to choose the value of N according to the characteristics of the wireless channel to avoid unnecessary complexity in the system design.

C. Hardware in the Loop Experimental Verification

To illustrate the proposed control structure and data transmission algorithm, an autonomous four-units test MG is implemented. The case study MG comprises four two-level three-phase 15 KVA power converters connected to the common bus through dedicated LC filters shown in Fig. 9.

In order to produce a power hardware in the loop (PHiL), a real time dSPACE MicroLabBox board is implemented. The setup parameters are tuned based on Table II and depicted in Fig. 9. The achievement of the proposed algorithm is shown in Fig. 10 where the dynamic response of the MG system
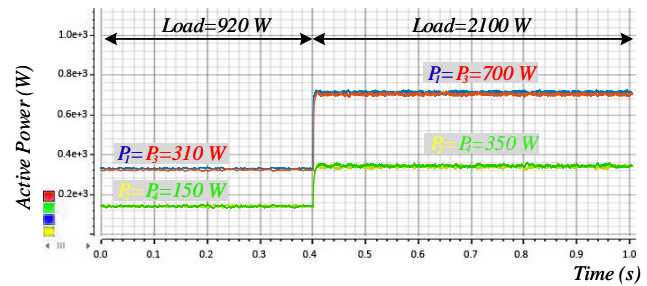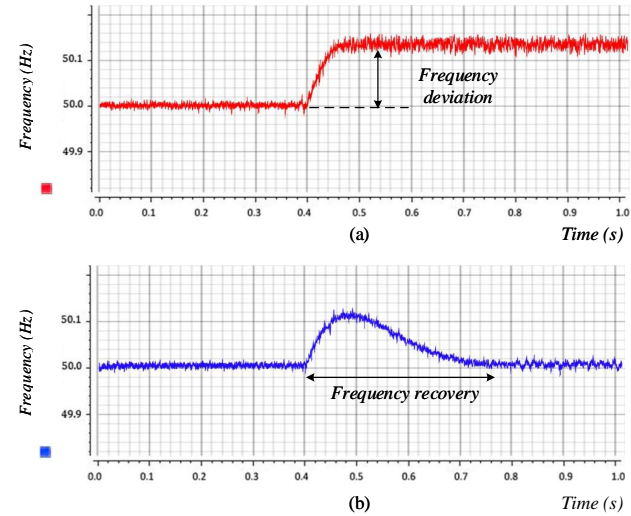

Fig. 11. Frequency regulation of the system under 60% packet loss: (a) without the prediction block (red), and (b) with data prediction block (blue).

is examined. Fig. 10 demonstrates fast and accurate power sharing among four VSCs in the presence of the proposed SC. Active power is shared properly when a load step change is enabled at $t = 0.4$ s. Accordingly, transient and steady state performance of power sharing are validated. Fig. 11 shows the impact of data transmission non-ideality when a load change is occurred. Fig. 11(a) and (b) demonstrate the secondary frequency control performance without (red) and with (blue) the proposed prediction block, respectively. In this scenario, data packet loss probability is set to 60%. As it can be seen, without the proposed data prediction block, the SC cannot restore the frequency properly. Due to the lack of acceptable data, the SC cannot generate a compensating signal and consequently, a steady frequency deviation can be seen in Fig. 11(a).

Nevertheless, the frequency is recovered in Fig. 11(b) where the proposed data prediction algorithm is activated. Similar to the simulation results, the experimental results have verified that fast and accurate frequency restoration is not achievable without the communication prediction block in the SC level considering communication non-ideality. The same results are achieved for secondary voltage control, which is shown in Fig. 12. With 60% data drop out probability, and without data prediction block, the SC cannot compensate for voltage deviations caused by PC and load change (Fig. 12(a)). However,
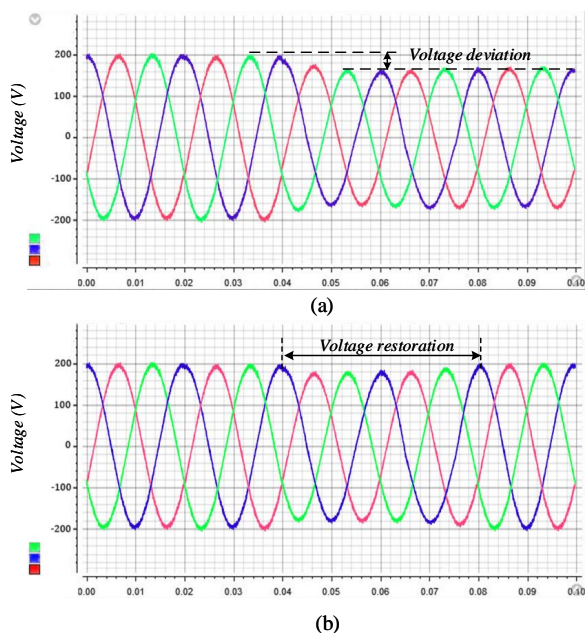
Fig. 12. Voltage regulation of the system under 60% packet loss: (a) without the data prediction block, and (b) with data prediction block.

by implementing the proposed CCB at SC level, the voltage amplitude deviations are restored accurately (Fig. 12(b)).

VI. CONCLUSION

This paper proposes a communication compensation block for secondary control of microgrids, primary controlled by FCS-MPC, to guarantee fast frequency and voltage restoration in the presence of communication impairments. The key idea in FCS-MPC is to embed all the inner loops of the PC level within a single control loop. This approach allows to design the secondary voltage and frequency control in a higher BW, which requires a faster data exchange. Therefore, as the main state-of-the-art of the paper, a communication compensation block is employed in the SC level to minimize and mitigate the communication impairments and non-idealities. The communication link deficiencies is mitigated by the proposed CCB which employs the prediction, estimation and finally decision algorithms on transmitted data. The robust data prediction algorithm based on the temporal and spatial correlation is applied to the SC to compensate for data drop-outs. Furthermore, the effect of the number of stored packets and burst packet loss on the average success rate of the communication block, and the small signal stability analysis of the system in the presence of the CCB is investigated. This modification not only enhances the dynamic performance of the MG, but also improves the system speed and robustness compared to the conventional methods. Simulation and power hardware-in-the-loop (PHiL) experimental results have verified that the proposed approach compensates very fast for frequency and voltage deviations and show the merits and applicability of the proposed method.

REFERENCES

[1] H. Bevrani, B. François, and T. Ise, *Microgrid dynamics and control.* John Wiley & Sons, 2017.

[2] A. Bidram and A. Davoudi, "Hierarchical structure of microgrids control system," *IEEE Trans. Smart Grid*, vol. 3, no. 4, pp. 1963–1976, 2012.

[3] H. Han, X. Hou, J. Yang, J. Wu, M. Su, and J. M. Guerrero, "Review of power sharing control strategies for islanding operation of ac microgrids," *IEEE Trans. Smart Grid*, vol. 7, no. 1, pp. 200–215, 2016.

[4] Q. Shafiee, J. M. Guerrero, and J. C. Vasquez, "Distributed secondary control for islanded microgrids—a novel approach," *IEEE Trans. Power Electrons.*, vol. 29, no. 2, pp. 1018–1031, Feb 2014.

[5] R. Heydari, T. Dragicevic, and F. Blaabjerg, "Coordinated operation of vscs controlled by mpc and cascaded linear controllers in power electronic based ac microgrid," in *Proc. IEEE COMPEL*, 2018, pp. 1–4.

[6] Y. Han, H. Li, P. Shen, E. A. A. Coelho, and J. M. Guerrero, "Review of active and reactive power sharing strategies in hierarchical controlled microgrids," *IEEE Trans. Power Electron.*, vol. 32, no. 3, pp. 2427–2451, 2017.

[7] K. E. Antoniadou-Plytaria, I. N. Kouveliotis-Lysikatos, P. S. Georgilakis, and N. D. Hatziargyriou, "Distributed and decentralized voltage control of smart distribution networks: models, methods, and future research," *IEEE Trans. Smart Grid*, vol. 8, no. 6, pp. 2999–3008, 2017.

[8] S. Liu, X. Wang, and P. X. Liu, "Impact of communication delays on secondary frequency control in an islanded microgrid," *IEEE Trans. Ind. Electron*, vol. 62, no. 4, pp. 2021–2031, 2015.

[9] Y. Han, K. Zhang, H. Li, E. A. A. Coelho, and J. M. Guerrero, "Mas-based distributed coordinated control and optimization in microgrid and microgrid clusters: a comprehensive overview," *IEEE Trans. Power Electron.*, vol. 33, no. 8, pp. 6488–6508, 2018.

[10] Y. Khayat, M. Naderi, Q. Shafiee, Y. Batmani, M. Fathi, J. M. Guerrero, and H. Bevrani, "Decentralized optimal frequency control in autonomous microgrids," *IEEE Trans. Power Syst.*, vol. 34, no. 3, pp. 2345–2353, 2018.

[11] J. Schiffer, T. Seel, J. Raisch, and T. Sezi, "Voltage stability and reactive power sharing in inverter-based microgrids with consensus-based distributed voltage control," *IEEE Trans. Control Syst. Technol.*, vol. 24, no. 1, pp. 96–109, 2016.

[12] Q. Shafiee, J. M. Guerrero, and J. C. Vasquez, "Distributed secondary control for islanded microgrids—a novel approach," *IEEE Trans. Power Electron.*, vol. 29, no. 2, pp. 1018–1031, 2014.

[13] J. Schiffer, F. Dörfler, and E. Fridman, "Robustness of distributed averaging control in power systems: Time delays & dynamic communication topology," *Automatica*, vol. 80, pp. 261–271, 2017.

[14] Q. Shafiee, C. Stefanovic, T. Dragicevic, P. Popovski, J. C. Vasquez, and J. M. Guerrero, "Robust networked control scheme for distributed secondary control of islanded microgrids," *IEEE Trans. Ind. Electron*, vol. 61, no. 10, pp. 5363–5374, 2014.

[15] J. W. Simpson-Porco, Q. Shafiee, F. Dörfler, J. C. Vasquez, J. M. Guerrero, and F. Bullo, "Secondary frequency and voltage control of islanded microgrids via distributed averaging," *IEEE Trans. Ind. Electron*, vol. 62, no. 11, pp. 7025–7038, 2015.

[16] A. Bidram, A. Davoudi, F. L. Lewis, and J. M. Guerrero, "Distributed cooperative secondary control of microgrids using feedback linearization," *IEEE Trans. Power Syst.*, vol. 28, no. 3, pp. 3462–3470, 2013.

[17] R. Han, L. Meng, G. Ferrari-Trecate, E. A. A. Coelho, J. C. Vasquez, and J. M. Guerrero, "Containment and consensus-based distributed coordination control to achieve bounded voltage and precise reactive power sharing in islanded ac microgrids," *IEEE Trans. Ind. Appl.*, vol. 53, no. 6, pp. 5187–5199, 2017.

[18] C. Li, E. A. A. Coelho, T. Dragicevic, J. M. Guerrero, and J. C. Vasquez, "Multiagent-based distributed state of charge balancing control for distributed energy storage units in ac microgrids," *IEEE Trans. Ind. Appl.*, vol. 53, no. 3, pp. 2369–2381, 2017.

[19] X. Wu, C. Shen, and R. Iravani, "A distributed, cooperative frequency and voltage control for microgrids," *IEEE Trans. Smart Grid*, vol. 9, no. 4, pp. 2764–2776, 2018.

[20] Q. Shafiee, V. Nasirian, J. C. Vasquez, J. M. Guerrero, and A. Davoudi, "A multi-functional fully distributed control framework for ac microgrids," *IEEE Trans. Smart Grid*, vol. 9, no. 4, pp. 3247–3258, 2018.

[21] H. Cai and G. Hu, "Distributed nonlinear hierarchical control of ac microgrid via unreliable communication," *IEEE Trans. Smart Grid*, vol. 9, no. 4, pp. 2429–2441, 2018.

[22] A. Pilloni, A. Pisano, and E. Usai, "Robust finite-time frequency and voltage restoration of inverter-based microgrids via sliding-mode cooperative control," *IEEE Trans. Ind. Electron.*, vol. 65, no. 1, pp. 907–917, 2018.

[23] T. Dragičević, "Model predictive control of power converters for robust and fast operation of ac microgrids," *IEEE Trans. Power Electron.*, vol. 33, no. 7, pp. 6304–6317, 2018.

[24] T. Dragičević, R. Heydari, and F. Blaabjerg, "Super-high bandwidth secondary control of ac microgrids," in *Proc. IEEE APEC*, 2018, pp. 3036–3042.

[25] R. Heydari, T. Dragicevic, and F. Blaabjerg, "High-bandwidth secondary voltage and frequency control of vsc-based ac microgrid," *IEEE Transactions on Power Electronics*, vol. 34, no. 11, pp. 11 320–11 331, 2019.

[26] E. A. A. Coelho, D. Wu, J. M. Guerrero, J. C. Vasquez, T. Dragičević, Č. Stefanović, and P. Popovski, "Small-signal analysis of the microgrid secondary control considering a communication time delay," *IEEE Trans. Ind. Electron.*, vol. 63, no. 10, pp. 6257–6269, 2016.

[27] H. Liang, B. J. Choi, W. Zhuang, and X. Shen, "Stability enhancement of decentralized inverter control through wireless communications in microgrids," *IEEE Trans. Smart Grid*, vol. 4, no. 1, pp. 321–331, 2013.

[28] W. Liu, W. Gu, W. Sheng, X. Meng, Z. Wu, and W. Chen, "Decentralized multi-agent system-based cooperative frequency control for autonomous microgrids with communication constraints," *IEEE Trans. Sustainable Energy*, vol. 5, no. 2, pp. 446–456, 2014.

[29] C. Ahumada, R. Cárdenas, D. Saez, and J. M. Guerrero, "Secondary control strategies for frequency restoration in islanded microgrids with consideration of communication delays," *IEEE Trans. Smart Grid*, vol. 7, no. 3, pp. 1430–1441, 2016.

[30] F.-L. Lian, J. Moyne, and D. Tilbury, "Network design consideration for distributed control systems," *IEEE Trans. Control Syst. Techn.*, vol. 10, no. 2, pp. 297–307, 2002.

[31] H. Fang, Z. Wu, and J. Wei, "Improvement for consensus performance of multi-agent systems based on weighted average prediction," *IEEE Trans. Autom. Control*, vol. 57, no. 1, pp. 249–254, 2012.

[32] Z. Wu, H. Fang, and Y. She, "Weighted average prediction for improving consensus performance of second-order delayed multi-agent systems," *IEEE Trans. Syst., Man, Cybern. B, Cybern.*, vol. 42, no. 5, pp. 1501–1508, 2012.

[33] C.-L. Lai and P.-L. Hsu, "Design the remote control system with the time-delay estimator and the adaptive smith predictor," *IEEE Trans. Ind. Informat*, vol. 6, no. 1, pp. 73–80, 2010.

[34] S. Ci, J. Qian, D. Wu, and A. Keyhani, "Impact of wireless communication delay on load sharing among distributed generation systems through smart microgrids," *IEEE Trans. Wireless Commun.*, vol. 19, no. 3, pp. 24–29, 2012.

[35] G. Lou, W. Gu, Y. Xu, W. Jin, and X. Du, "Stability robustness for secondary voltage control in autonomous microgrids with consideration of communication delays," *IEEE Trans. Power Syst.*, vol. 33, no. 4, pp. 4164–4178, 2018.

[36] S. Bukowski and S. Ranade, "Communication network requirements for the smart grid and a path for an ip based protocol for customer driven microgrids," in *2012 IEEE Energytech*. IEEE, 2012, pp. 1–6.

[37] J. R. Klotz, S. Obuz, Z. Kan, and W. E. Dixon, "Synchronization of uncertain euler–lagrange systems with uncertain time-varying communication delays," *IEEE Trans. Cybern.*, vol. 48, no. 2, pp. 807–817, 2018.

[38] X. Lu, X. Yu, J. Lai, J. M. Guerrero, and H. Zhou, "Distributed secondary voltage and frequency control for islanded microgrids with uncertain communication links," *IEEE Trans. Ind. Informat.*, vol. 13, no. 2, pp. 448–460, 2017.

[39] K. Yousef, Q. Shafiee, R. Heydari, M. Naderi, T. Dragicevic, J. W. Simpson-Porco, F. Dorfler, M. Fathi, F. Blaabjerg, J. M. Guerrero *et al.*, "On the secondary control architectures of ac microgrids: An overview," *IEEE Trans. Power Electrons.*, 2019.

[40] J. Fang, Z. Shuai, X. Zhang, X. Shen, and Z. J. Shen, "Secondary power sharing regulation strategy for a dc microgrid via maximum loading factor," *IEEE Trans. Power Electrons.*, vol. 34, no. 12, pp. 11 856–11 867, Dec 2019.

[41] P. C. Loh, D. Li, Y. K. Chai, and F. Blaabjerg, "Hybrid ac–dc microgrids with energy storages and progressive energy flow tuning," *IEEE Trans. Power Electrons.*, vol. 28, no. 4, pp. 1533–1543, April 2013.

[42] S. Moayedi and A. Davoudi, "Unifying distributed dynamic optimization and control of islanded dc microgrids," *IEEE Trans. Power Electrons*, vol. 32, no. 3, pp. 2329–2346, March 2017.

[43] W. Yu, T. L. Nguyen, Y. Xu, Z. Li, Q.-T. Tran, and R. Caire, "Cyber-physical design and implementation of distributed event-triggered secondary control in islanded microgrids," *IEEE Trans. Ind. Appl.*, vol. 55, no. 6, pp. 5631–5642, 2019.

[44] V. Venkatesh, A. K. Srivastava, A. Hahn, and S. Zonouz, "Measuring and enhancing microgrid resiliency against cyber threats," *IEEE Trans. Ind. Appl.*, vol. 55, no. 6, pp. 6303–6312, 2019.

[45] L. Zhiyi, S. Mohammad, and F. Aminifar, "Cybersecurity in distributed power systems," *Proceedings of the IEEE*, vol. 105, no. 7, pp. 1367–1388, 2017.

[46] R. Olfati-Saber, J. A. Fax, and R. M. Murray, "Consensus and cooperation in networked multi-agent systems," *Proc. of the IEEE*, vol. 95, no. 1, pp. 215–233, 2007.

[47] Q.-C. Zhong, "Robust droop controller for accurate proportional load sharing among inverters operated in parallel," *IEEE Trans. Ind. Electron*, vol. 60, no. 4, pp. 1281–1290, 2013.

[48] R. Bruno, M. Conti, and E. Gregori, "Throughput analysis and measurements in ieee 802.11 wlans with tcp and udp traffic flows," *IEEE Trans. Mobile Comput.*, vol. 7, no. 2, pp. 171–186, Feb 2008.

[49] J. J. Nielsen, R. Liu, and P. Popovski, "Ultra-reliable low latency communication using interface diversity," *IEEE Trans. Commun.*, vol. 66, no. 3, pp. 1322–1334, 2018.

[50] P. Popovski, J. J. Nielsen, C. Stefanovic, E. De Carvalho, E. Strom, K. F. Trillingsgaard, A.-S. Bana, D. M. Kim, R. Kotaba, J. Park *et al.*, "Wireless access for ultra-reliable low-latency communication: Principles and building blocks," *Ieee Network*, vol. 32, no. 2, pp. 16–23, 2018.

[51] T. Dragicevic, M. Lu, and F. Blaabjerg, "Improved model predictive control for high voltage quality in ups applications," in *Proc. IEEE ECCE*, Sept 2017, pp. 1–7.

Rasool Heydari (S'16-M'19) received the Ph.D. degree in electrical engineering from the Department of Energy Technology, Aalborg University, Denmark, in 2019, where he focused on several research activities related to power electronic based power systems, under the supervision of Prof. F. Blaabjerg. He was also a visiting researcher with ABB Corporate Research Center, Västerås, Sweden, in 2019. He is currently a Post-Doctoral Fellow with the Department of Electrical Engineering, the Mads Clausen Institute, University of Southern Denmark, Odense, Denmark. His principal field of interest include control, stability and dynamic analysis of power electronic systems, mainly distributed and grid-connected converters, microgrid, and low-inertia power grids. Dr. Heydari serves as a Reviewer with several journals, including IEEE Transactions on Power Electronics, the IEEE Transactions on Industrial Electronics, and the IET Power Electronics.

Yousef Khayat (S' 16) received the B.Sc. degree from Urmia University, Urmia, Iran, and the M.Sc. (Hons.) degree from the Iran University of Science and Technology (IUST), Tehran, Iran, both in electrical engineering, in 2012 and 2014, respectively. He is currently working toward the Ph.D. degree in Electrical Engineering at Aalborg University, Aalborg, Denmark. His research interests include Microgrid dynamics and control, robust, predictive, and nonlinear control for application of power electronics in distributed systems.

Abolfazl Amiri received his B.S. degree in Electrical and Communications Engineering (with honors) from University of Tabriz, Tabriz, Iran in 2013, and M.S. degree in Electrical and Communication Systems Engineering, from University of Tehran, Tehran, Iran in 2016. He is currently a PhD fellow in Electronic systems department of Aalborg University, Aalborg, Denmark. He was with Huawei technologies Tehran office from 2016 to 2017 as an RF engineer and cellular network optimizer. His research interests include applications of signal processing and machine learning in wireless communications and multi-antenna systems.

Tomislav Dragicevic (S'09-M'13-SM'17) received the M.Sc. and the industrial Ph.D. degrees in Electrical Engineering from the Faculty of Electrical Engineering, University of Zagreb, Croatia, in 2009 and 2013, respectively. From 2013 until 2016 he has been a Postdoctoral researcher at Aalborg University, Denmark. From March 2016 until March 2020 he was an Associate Professor at Aalborg University, Denmark. From April 2020 he is a Professor at the Technical University of Denmark. He made a guest professor stay at Nottingham University, UK during spring/summer of 2018. His research interest is application of advanced control, optimization and artificial intelligence inspired techniques to provide innovative and effective solutions to emerging challenges in design, control and cyber-security of power electronics intensive electrical distributions systems and microgrids. He has authored and co-authored more than 220 technical publications (more than 100 of them are published in international journals, mostly in IEEE), 8 book chapters and a book in the field. He serves as an Associate Editor in the IEEE TRANSACTIONS ON INDUSTRIAL ELECTRONICS, in IEEE TRANSACTIONS ON POWER ELECTRONICS, in IEEE Emerging and Selected Topics in Power Electronics and in IEEE Industrial Electronics Magazine. Dr. Dragičević is a recipient of the Končar prize for the best industrial PhD thesis in Croatia, a Robert Mayer Energy Conservation award, and he is a winner of an Alexander von Humboldt fellowship for experienced researchers. He is currently listed as one of the top 5 trending authors in Engineering globally by Microsoft Academic.

Frede Blaabjerg (S'86-M'88-SM'97-F'03) was with ABB-Scandia, Randers, Denmark, from 1987 to 1988. From 1988 to 1992, he got the PhD degree in Electrical Engineering at Aalborg University in 1995. He became an Assistant Professor in 1992, an Associate Professor in 1996, and a Full Professor of power electronics and drives in 1998. From 2017 he became a Villum Investigator. He is honoris causa at University Politehnica Timisoara (UPT), Romania and Tallinn Technical University (TTU) in Estonia. His current research interests include power electronics and its applications such as in wind turbines, PV systems, reliability, harmonics and adjustable speed drives. He has published more than 600 journal papers in the fields of power electronics and its applications. He is the co-author of four monographs and editor of ten books in power electronics and its applications. He has received 32 IEEE Prize Paper Awards, the IEEE PELS Distinguished Service Award in 2009, the EPE-PEMC Council Award in 2010, the IEEE William E. Newell Power Electronics Award 2014, the Villum Kann Rasmussen Research Award 2014, the Global Energy Prize in 2019 and the 2020 IEEE Edison Medal. He was the Editor-in-Chief of the IEEE TRANSACTIONS ON POWER ELECTRONICS from 2006 to 2012. He has been Distinguished Lecturer for the IEEE Power Electronics Society from 2005 to 2007 and for the IEEE Industry Applications Society from 2010 to 2011 as well as 2017 to 2018. In 2019-2020 he serves a President of IEEE Power Electronics Society. He is Vice-President of the Danish Academy of Technical Sciences too. He is nominated in 2014-2019 by Thomson Reuters to be between the most 250 cited researchers in Engineering in the world.

Qobad Shafiee (S'13-M'15-SM'17) received PhD degree in electrical engineering from the Department of Energy Technology, Aalborg University (Denmark) in 2014. He is currently an Assistant Professor, Director of International Affairs, and Co-Leader of the Smart/Micro Grids Research Center at the University of Kurdistan (Sanandaj, Iran), where he was a lecturer from 2007 to 2011. In 2014, he was a Visiting Scholar with the Electrical Engineering Department, the University of Texas at Arlington, Arlington, TX, USA. He was a Post-Doctoral Fellow with the Department of Energy Technology, Aalborg University in 2015. His current research interests include modeling, energy management, control of power electronics-based systems and microgrids, and model predictive and optimal control of modern power systems.

Petar Popovski (S'97-M'04-SM'10-F'16) is a Professor at Aalborg University, where he is heading the section on Connectivity. He received his Dipl. Ing and M. Sc. degrees in communication engineering from the University of Sts. Cyril and Methodius in Skopje and the Ph.D. degree from Aalborg University in 2005. He is a Fellow of IEEE, has over 300 publications in journals, conference proceedings, and edited books and he was featured in the list of Highly Cited Researchers 2018, compiled by Web of Science. He holds over 30 patents and patent applications. He received an ERC Consolidator Grant (2015), the Danish Elite Researcher award (2016), IEEE Fred W. Ellersick prize (2016), IEEE Stephen O. Rice prize (2018) and the Technical Achievement Award from the IEEE Technical Committee on Smart Grid Communications. He is currently a Steering Committee Member of IEEE SmartGridComm and IEEE Transactions on Green Communications and Networking. He previously served as a Steering Committee Member of the IEEE INTERNET OF THINGS JOURNAL. He is currently an Area Editor of the IEEE TRANSACTIONS ON WIRELESS COMMUNICATIONS. Prof. Popovski was the General Chair for IEEE SmartGridComm 2018 and IEEE Communication Theory Workshop 2019. From 2019, he is also a Member-at-Large of the Board of Governors of the IEEE Communications Society. His research interests are in the area of wireless communication, communication theory and Internet of Things.